Research Square

Preprints are preliminary reports that have not undergone peer review.
They should not be considered conclusive, used to inform clinical practice,
or referenced by the media as validated information.

Nitrogen and plant density reshape the allometric basis of morphological lodging resistance potential in maize

Jianbo Shen
Wenzhou Vocational College of Science and Technology
Chao Bai
Ningbo Institute of Surveying
Ning Zhang
Henan Yuanzhi Forestry Planning and Design Co., Ltd
Mengli L. Zhou
mlzhou@henau.edu.cn

Henan Agricultural University
Guo Fang
Henan Agricultural University
Dongfeng Yan
Henan Agricultural University
Simon X. Yang
University of Guelph

Research Article

Keywords: Zea mays L., stem diameter-height allometry, Euler buckling, nitrogen × density interaction, mixed-effects model

Posted Date: November 3rd, 2026

DOI: https://doi.org/10.21203/rs.3.rs-11320414/v1

License: This work is licensed under a Creative Commons Attribution 4.0 International License.
Read Full License

Additional Declarations: No competing interests reported.

Nitrogen and plant density reshape the allometric basis of morphological lodging resistance potential in maize

Jianbo Shen[1], Chao Bai[2], Ning Zhang[3], Mengli Zhou[4]*,Guo Fang[4], Dongfeng Yan[4], Simon X. Yang[5]

1.Wenzhou Key Laboratory of AI Agents for Agriculture, Wenzhou Vocational College of Science and Technology, Wenzhou 325006, China

2. Ningbo Institute of Surveying,Mapping And Remote Sensing, Ningbo, Zhejiang 315042, China

3. Henan Yuanzhi Forestry Planning and Design Co., Ltd, Zhengzhou, Henan, 450003, China

4. College of Forestry, Henan Agricultural University, Zhengzhou, Henan, 450046, China

5. Advanced Robotics and Intelligent Systems Laboratory, College of Engineering, University of Guelph, N1G 2W1, Canada.

*Correspondence: mlzhou@henau.edu.cn (M. L. Zhou)

Abstract: Lodging remains a major constraint to maize (*Zea mays* L.) productivity worldwide. Stem diameter (D) and plant height (H) jointly determine stalk mechanical stability through an allometric relationship rooted in Euler buckling theory, yet how nitrogen and plant density reshape this allometric basis across commercial hybrids remains poorly quantified. We analyzed a TerraSentia robot-based phenotyping data from a nitrogen × density × hybrid field experiment and computed the morphological lodging resistance index (MLRI = D^4/H^2) for 370 plant-level observations from six commercial hybrids across four nitrogen rates (0–336kg N·ha^{-1}) and three plant density classes. Linear mixed-effects models with hybrid as random intercept were used to partition the effects of *ln*(D), nitrogen, density, and their interactions, with model comparison by AIC/BIC on a common sample. The best model (*ln* (D) × N + density, marginal $R^2 = 0.946$, conditional $R^2 = 0.980$, LOOCV $R^2 = 0.923$) revealed a dominant positive effect of stem diameter ($\beta = 3.729$, $p < 2\times10^{-16}$) and significant negative nitrogen main effects (−0.88 to −1.07, all $p < 0.001$) that were partially reversed by positive *ln* (D) × N interactions (0.232 to 0.293, all $p < 0.01$). Plant density showed contrasting patterns: simple group means declined from 12.4 (low) to 7.6 (high), yet the

partial coefficient was positive (+0.077, $p < 2\times10^{-16}$), indicating two independent pathways—an indirect one via reduced stem diameter and a direct one via suppressed plant height. Hybrid identity explained 67% of unexplained variance (ICC = 0.671), with 13 of 15 pairwise comparisons significant after Tukey adjustment. Three MLRI formulations (D^4/H^2, D^3/H, D^2/H) yielded nearly identical rankings (Spearman $\rho\geq0.994$) and qualitatively identical coefficients, confirming robustness. The result demonstrate that nitrogen and plant density shift the allometric balance of morphological lodging resistance through partially independent pathways, and that D^4/H^2 provides a rapid, robot-phenotyping-compatible morphological proxy that may complement mechanical and field-based lodging assessments.

Keywords: *Zea mays* L.; stem diameter-height allometry; Euler buckling; nitrogen × density interaction; mixed-effects model

1 Introduction

Maize (*Zea mays* L.) is one of the three most important cereal crops worldwide, providing food, feed, and industrial raw materials for billions of people. Global maize production has increased steadily over the past decades, largely driven by higher planting densities and greater nitrogen inputs [1,2]. However, these intensification practices have also increased the risk of stalk lodging, the permanent displacement of stems from vertical—which causes an estimated 5–20% annual yield loss worldwide and up to 60% under extreme weather events [3-5]. Lodging not only reduces harvestable yield but also interferes with mechanical harvesting, increases grain moisture at harvest, and reduces grain quality [6,7]. Improving lodging resistance has therefore become a central objective in maize breeding and agronomic management.

Lodging resistance is a complex trait determined by the interaction of stalk mechanical strength, stem morphology, root anchorage, and canopy architecture [8,9]. Among these components, stem morphology plays a particularly important role because it can be measured non-destructively and at high throughput. Direct mechanical phenotyping, such as rind penetrometer resistance or three-point bending tests, provides accurate estimates of stalk strength but is destructive, labor-intensive, and incompatible with the large populations used in modern breeding programs [10,11]. Morphological

indices offer an attractive alternative, provided they are grounded in a clear physical model.

Euler's buckling theory provides such a model. For a cylindrical stem of uniform elastic modulus, the critical buckling load scales as:

$$P_{cr} \propto \frac{E \times D^4}{H^2} \quad (1)$$

where E is the elastic modulus of stem tissue, D is stem diameter, and H is plant height. This relationship defines the morphological lodging resistance index (MLRI = D^4/H^2), which has been applied across cereals including wheat [3], maize [12], and rice [13]. MLRI captures the fundamental allometric trade-off between radial thickening and vertical elongation, a trade-off that determines whether a plant invests resources in mechanical stability or in light capture [14-16]. Because both D and H can be obtained from the same non-destructive measurements already collected by many high-throughput phenotyping platforms, MLRI is a cost-effective addition to existing breeding pipelines [17-19].

The allometric basis of MLRI is not fixed. Both nitrogen and plant density, the two dominant agronomic drivers of maize canopy architecture, are known to shift the relationship between stem diameter and plant height, but their effects are complex and partially opposing [20,21]. Nitrogen typically increases both stem diameter and plant height, yet the allometric exponent relating them often declines under high nitrogen availability, producing relatively taller, thinner stems [22,23]. This shift can reduce mechanical stability per unit stem diameter, even as absolute stem thickness increases. Plant density has an even more complex effect: increasing density reduces per-plant stem diameter through inter-plant competition for light, water, and nutrients, but it also suppresses plant height through shade-avoidance responses and resource limitation [24,25]. The net effect on MLRI depends on the relative magnitudes of these two pathways, which may differ across genotypes and environments [26].

Despite decades of research on nitrogen and plant density individually, three important gaps remain in our understanding of how they jointly reshape morphological lodging resistance. First, most studies examine stem diameter and plant height as

independent traits rather than as components of an integrated allometric index [27,28]. This limits our ability to translate morphological variation into predictions of mechanical stability, because the two traits interact multiplicatively through the D^4/H^2 relationship. Second, the combined effect of nitrogen and density on the allometric basis of lodging resistance has rarely been quantified in a mixed-effects framework that properly separates genotype, environment, and their interaction [23,29]. Without such a framework, the relative contributions of treatment effects and genetic variation cannot be disentangled, and hybrid-specific responses may be confounded with block or replicate effects. Third, previous analyses typically rely on small, single-treatment designs that cannot simultaneously estimate the independent contributions of nitrogen, density, and hybrid identity, nor test whether nitrogen effects depend on stem diameter [30,31].

Here we address these gaps by asking: how do nitrogen and plant density jointly reshape the allometric basis of morphological lodging resistance in maize? Using a publicly available TerraSentia robot-based phenotyping data from a nitrogen × density × hybrid field experiment, we computed the morphological lodging resistance index ($MLRI = D^4/H^2$) and fitted linear mixed-effects models to partition the contributions of stem diameter, nitrogen, density, and their interactions. Our objectives were threefold: (i) to quantify the independent and interactive effects of stem diameter, nitrogen, and plant density on MLRI, with particular attention to whether nitrogen effects depend on stem diameter; (ii) to partition the variance attributable to hybrid identity and test pairwise differences among hybrids using estimated marginal means with Tukey adjustment; and (iii) to assess the robustness of conclusions across three alternative MLRI formulations (D^4/H^2, D^3/H, D^2/H) through multicollinearity diagnostics, residual analysis, and leave-one-out cross-validation. We hypothesized that (H1) nitrogen would exert a dual effect on MLRI, negative at fixed stem diameter but positive via increased stem diameter, producing a net positive effect across the nitrogen gradient; and (H2) plant density would show contrasting simple and partial effects, reflecting an indirect negative pathway via reduced stem diameter and a direct positive pathway via suppressed plant height. We further expected that stem diameter would dominate MLRI,

consistent with the D^4 dependence in Euler buckling theory, and that hybrid identity would explain a substantial portion of residual variance with stable rankings across nitrogen levels.

2 Material and Methods

2.1 Data source and experimental design

Phenotypic data were obtained from the publicly available Dryad Digital Repository (DOI: 10.5061/dryad.bnzs7h4f1), corresponding to a nitrogen × density × hybrid (N×D×H) field experiment conducted at the Windfall research station in Indiana, USA, during the 2022 growing season. The dataset (Sheet "Figure 2") contains plant-level morphological measurements collected with a TerraSentia robot phenotyping platform on 29 July 2022, at the late vegetative stage (approximately V12–V14).

Six commercial maize hybrids (P0825AM, P1093Q, P1108Q, P1213YHR, P1366YHRCC, and P1442YHRCE) were evaluated across a factorial combination of four nitrogen rates and three target plant densities. Nitrogen was applied as urea ammonium nitrate at rates of 0, 112, 224, and 336 kg N·ha^{-1} (corresponding to the original dataset values of 0, 100, 200, and 300 lbs N·acre^{-1}; 1 lb acre^{-1} ≈ 1.12085 kg·ha^{-1}). Target plant densities were 44,500, 69,200, and 118,600 plants·ha^{-1} (equivalent to 4.45, 6.92, and 11.86 plants·m^{-2}, and corresponding to the original dataset values of 18,000, 28,000, and 48,000 plants·acre^{-1}). The experiment was arranged with four replicates; each plot was uniquely identified by Replicate, Plot, and Range within the field. Detailed agronomic management, soil characteristics, and site description are available in the original dataset documentation.

Two morphological traits were extracted from the TerraSentia-based measurements of stem diameter and plant height: stem diameter (D, mm) and plant height (H, cm), recorded as STD29July and PLTHT29July in the original dataset, respectively. Additional variables used for modeling were: nitrogen rate (four-level factor: 0, 112, 224, 336 kg N·ha^{-1}), observed plant density (plants·m^{-2}), hybrid identity (six-level factor), and replicate (four-level factor).

2.2 Morphological lodging resistance index (MLRI) and derived variables

The morphological lodging resistance index (MLRI) was defined following Euler

buckling theory. For a cylindrical stem of uniform elastic modulus, the critical buckling load (P_{cr}) scales with the fourth power of stem diameter and inversely with the square of plant height (Eq. 2).

$$P_{cr} \propto \frac{E \times D^4}{H^2} \quad (2)$$

where P_{cr} is the critical buckling load (the maximum load a stem can withstand before buckling), E is the elastic modulus of stem tissue, D is stem diameter, and H is plant height. Because E cannot be measured non-destructively, the morphological component of this relationship was retained as the MLRI (Eq. 3).

$$MLRI = \frac{D^4}{H^2} \quad (3)$$

where D is expressed in mm and H in cm. To evaluate the sensitivity of our conclusions to the specific exponent, two alternative formulations were also compute $MLRI_{D3/H} = \frac{D^3}{H}$ and $MLRI_{D2/H} = \frac{D^2}{H}$. All three formulations were used in the robustness analysis.

Natural-logarithm transformations (*ln*, base *e*) were applied to all MLRI formulations to stabilize variance and to allow regression coefficients to be interpreted as approximate proportional changes. Unlike log_{10} transformations, natural-log transformations preserve the direct interpretation of coefficients as elasticities.

Two density-related variables were constructed to capture both continuous and categorical aspects of plant density. Standardized density was obtained by mean-centering observed plant density (plants·m^{-2}) and scaling to unit standard deviation, allowing the coefficient to be interpreted per one standard deviation change. A three-level density class variable was also constructed using natural break points in the observed density distribution: Low (< 7 plants·m^{-2}), Medium (7–9 plants·m^{-2}), and High (> 9 plants·m^{-2}). This categorical variable was used only for descriptive statistics and visualization, not for model fitting.

2.3 Linear mixed-effects models

Linear mixed-effects models were fitted using the "lme4" package [32] in R v4.4.1 [33]. The response variable was *ln*(MLRI) (Eq. 4). Fixed effects were *ln*(D), nitrogen rate (as a four-level factor), standardized density, and their interactions. Hybrid identity

was included as a random intercept to account for the repeated measurement of genotypes across treatments:

$$\ln(MLRI_{ij}) = \beta_0 + \beta_1 \times \ln(D_{ij}) + \beta_2 \times N_{ij} + \beta_3 \times [\ln(D_{ij}) \times N_{ij}] + \beta_4 \times Density_{ij} + u_{0i} + \varepsilon_{ij} \quad (4)$$

where $ln(D_{ij})$ is the natural logarithm of stem diameter for observation j in hybrid i; N_{ij} is the nitrogen rate factor with 0 kg N·ha^{-1} as the reference level; $ln(D_{ij}) \times N_{ij}$ denotes the statistical interaction between $ln(D)$ and N (following standard R formula notation; it is not algebraic multiplication); $Density_{ij}$ is the standardized density; $u_{0i} \sim N(0, \sigma_u^2)$ is the random intercept for hybrid i; and $\varepsilon_{ij} \sim N(0, \sigma^2)$ is the residual error.

A second random intercept for replicate was initially considered, but the model specification was simplified when the replicate variance component was found to be non-estimable under the boundary constraint. Following standard practice for mixed-effects model selection [34,35], the final model retained only the hybrid random intercept, as the simpler specification provided equivalent fit with fewer parameters and no convergence issues.

Six candidate models were fitted to assess the relative contributions of stem diameter, nitrogen, density, and their interactions (Table 1). Model m0 contained only the intercept; m1 added ln(D); m2 added nitrogen as a main effect; m3 introduced the ln(D) × N interaction; m4 further added standardized density; and m5 replaced the ln(D) × N interaction with ln(D) × density. To ensure comparability of information criteria, all candidate models were fitted on a common dataset containing observations with complete records for every predictor. The maximum-likelihood estimator was used for model comparison via AIC and BIC [36,37]; the restricted maximum-likelihood estimator was used for final parameter inference and hypothesis testing.

Statistical significance of fixed effects was assessed using Satterthwaite's approximation for denominator degrees of freedom, implemented in the “lmerTest” package. Type III sums of squares were used for all ANOVA tables to test the effect of each term after controlling for all other terms, including interactions.

Table 1. Candidate linear mixed-effects models for *ln*(MLRI).

Model	Fixed-effects structure
m0	Intercept only
m1	*ln*(D)
m2	*ln*(D) + N
m3	*ln*(D)× N
m4	*ln*(D) × N + Density
m5	*ln*(D) × Density + N

Note:All models included a random intercept for hybrid identity. The best-fitting model was selected by AIC and BIC on a common sample. *ln*(D) = natural logarithm of stem diameter (mm); *N* = nitrogen rate (four-level factor); Density = standardized plant density.

2.4 Post-hoc comparisons and variance partitioning

Hybrid marginal means and pairwise contrasts were obtained from a fixed-effects version of the best-fitting model using the "emmeans" package [38], with Tukey adjustment for multiple comparisons across all hybrid pairs [39]. A fixed-effects specification was used for post-hoc inference because with a small number of hybrids, random-effect variance components are estimated imprecisely and bootstrap confidence intervals become excessively wide.

The intraclass correlation coefficient (ICC) (Eq. 5) was computed to quantify the proportion of unexplained variance attributable to hybrid identity:

$$ICC=\frac{\sigma_u^2}{\sigma_u^2+\sigma^2} \tag{5}$$

where σ_u^2 is the hybrid random-intercept variance and σ^2 is the residual variance [40]. The ICC can be interpreted as the expected correlation between two observations drawn from the same hybrid. Pairwise contrasts were adjusted for multiple comparisons using the false discovery rate [41].

2.5 Model diagnostics, sensitivity, and validation

Multicollinearity among predictors was assessed using generalized variance inflation factors (GVIF) computed with the "car" package [42]. For terms with more than one degree of freedom (e.g., the four-level nitrogen factor), we report the adjusted statistic $GVIF_{adj}^{\left(\frac{1}{2df}\right)}$, as the diagnostic criterion [43]. A threshold of 1.5 was used to indicate absence of collinearity; values between 1.5 and 2 were considered moderate,

and values above 2 were considered problematic.

Four residual diagnostic plots were generated from the best-fitting model: residuals versus fitted values with a LOESS smoother, a normal Q-Q plot of standardized residuals, a histogram of residuals with normal overlay, and residuals versus *ln*(D). Formal tests included the Shapiro-Wilk test for normality [44]and the Breusch-Pagan test for homoscedasticity [45], implemented in the "lmtest" package.

Three robustness checks were performed to assess whether conclusions depend on specific analytical choices. The best-fitting model was re-fitted using ln($MLRI_{D3/H}$) and ln($MLRI_{D2/H}$) as alternative response variables. Coefficients for ln(D), nitrogen, density, and the ln(D) × N300 interaction were compared across the three formulations. Spearman rank correlations between the three MLRI formulations were also computed to confirm that genotype and treatment rankings were preserved. Leave-one-out cross-validation was performed on a fixed-effects version of the best model [46] (Stone, 1974). For each observation, the model was refitted with that observation held out, and the prediction error was recorded on the natural-log scale. Three metrics were reported: root mean squared error, mean absolute error, and the squared Pearson correlation between observed and predicted values. Cross-validation R^2 was compared to the marginal and conditional R^2 of the fitted model to assess overfitting. All candidate models were fitted on the same set of observations to ensure that AIC and BIC values were directly comparable. This required excluding any observation with a missing value for at least one predictor.

A random seed was set before all analyses involving random sampling or bootstrap procedures. Analysis scripts are available from the corresponding author upon reasonable request.

3 Results

3.1 Phenotypic variation and model selection

Stem diameter increased monotonically with nitrogen, from 25.8 ± 3.3 mm at 0 kg N·ha^{-1} to 28.6 ± 3.3 mm at 336 kg N·ha^{-1}, while plant height increased from 235 ± 18.9 cm to 250 ± 15.2 cm (Table 2). The derived MLRI rose from 8.63 ± 3.99 to 11.67 ± 5.43, representing a 35% increase across the nitrogen gradient. Plant height showed a

saturation pattern, with most of the increase occurring between 0 and 224 kg N·ha^{-1} (235 → 249 cm), whereas the 336 kg N·ha^{-1} treatment added only 0.6 cm on average.

Among the six candidate models, m1 (*ln*(D) only) already explained 91.5% of variance in *ln*(MLRI), confirming stem diameter as the dominant driver of morphological lodging resistance. Adding nitrogen (m2) and the *ln*(D) × N interaction (m3) improved fit marginally (marginal R^2 = 0.922 and 0.924, respectively). The largest improvement came from adding standardized density (m4), which reduced AIC by 232.4 units relative to m3 and raised marginal R^2 to 0.946 (Table 3). Model m5 performed similarly on fit (AIC = −945.5) but required an additional interaction term; m4 was therefore selected by parsimony.

The best-fitting model m4 achieved marginal R^2= 0.946 and conditional R^2= 0.980, indicating that fixed effects explained 94.6% of variance, with an additional 3.4% attributable to hybrid random effects. Cross-validation R^2= 0.923, RMSE = 0.126, and MAE = 0.099 on the natural-log scale (Table 4), indicating minimal overfitting. The joint distribution of stem diameter and plant height is shown in Figure S1.

Table 2 Descriptive statistics of stem diameter (D), plant height (H), and morphological lodging resistance index (MLRI = D^4/H^2) across four nitrogen rates

Nitrogen rate (kg N·ha^{-1})	*n*	Stem diameter (mm)	Plant height (cm)	MLRI (D^4/H^2)
0	93	25.8 ± 3.3	235.0 ± 18.9	8.63 ± 3.99
112	93	26.4 ± 3.1	244.4 ± 16.0	8.75 ± 4.22
224	93	27.0 ± 3.0	249.2 ± 14.1	9.12 ± 3.93
336	91	28.6 ± 3.3	249.8 ± 15.2	11.67 ± 5.43

Note: Values are means ± standard deviation. N = number of plant-level observations. D in mm; H in cm; MLRI in (mm^4·cm^{-2}).

Table 3 Comparison of six candidate linear mixed-effects models for *ln*(MLRI)

Model	Fixed-effects structure	AIC	BIC	Marginal R^2	Conditional R^2
m0	Intercept only	453.7	465.4	0	0.072
m1	*ln*(D)	−662.8	−647.2	0.915	0.955
m2	*ln*(D)+ N	−713.4	−686.0	0.922	0.962
m3	*ln*(D) × N	−717.9	−678.8	0.924	0.963
m4	*ln*(D) × N + Density	−950.3	−907.3	0.946	0.98
m5	*ln*(D) × Density + N	−945.5	−910.3	0.946	0.98

Note: All models were fitted on a common sample of *n* = 370 observations. The best-fitting model (m4) is shown in bold.

Table 4. Leave-one-out cross-validation (LOOCV) performance of the best-fitting model.

Metric	Value
RMSE (ln scale)	0.126
MAE (ln scale)	0.099
R^2	0.923

Note: LOOCV was performed on the fixed-effects version of the best model. RMSE = root mean squared error; MAE = mean absolute error; R^2= squared Pearson correlation between observed and predicted values.

3.2 Dual effects of nitrogen on the allometric basis

In the best model (Table 5), *ln*(D) had the strongest positive effect on *ln*(MLRI) (β = 3.729, SE = 0.057, $p < 2\times10^{-16}$), consistent with the D^4 dependence of Euler buckling. This coefficient indicates that a 1% increase in stem diameter was associated with approximately a 3.73% increase in MLRI, demonstrating that radial thickening is the primary mechanism through which plants achieve morphological lodging resistance.

Nitrogen showed a negative main effect across all levels relative to the 0 kg N·ha^{-1} control: $\beta = -0.930$ for 112 kg N·ha^{-1}, $\beta = -1.069$ for 224 kg N·ha^{-1}, and $\beta = -0.879$ for 336 kg N·ha^{-1} (all $p < 0.001$). At a fixed stem diameter, higher nitrogen reduced MLRI by 0.88–1.07 ln units, equivalent to a 15–22% reduction on the original scale.

However, nitrogen also showed a positive *ln*(D) × N interaction across all levels: +0.262, +0.293, and +0.232 for 112, 224, and 336 kg N·ha^{-1}, respectively (all $p < 0.01$). These positive interactions indicate that the negative nitrogen main effect weakened as stem diameter increased, that is, nitrogen's suppressive effect on MLRI was partially offset in thicker-stemmed plants.

The combination of negative main effects and positive interactions reveals a dual mechanism. At a fixed stem diameter, higher nitrogen reduced MLRI, consistent with nitrogen-driven internode elongation increasing plant height disproportionately. But nitrogen also increased stem diameter by 2.8 mm on average from 0 to 336 kg N·ha^{-1}, and this increase dominated the net effect through the D^4 term. The result was a net positive MLRI increase of 35% across the nitrogen gradient (Table 6, Figure 1).All main effects and the *ln*(D) × N interaction as significant: *ln* D ($F_{1,356}$ = 11527.2, $p <$

310 2.2×10^{-16}), nitrogen rate ($F_{3,356} = 7.66$, $p < 0.001$), density ($F_{1,356} = 321.2$, $p < 2.2\times10^{-16}$), and *ln* D × N ($F_{3,356} = 6.13$, $p < 0.001$). The relationship between ln(MLRI) and stem diameter or plant height is shown in Figure S2.

313 **Table 5** Fixed-effect coefficients of the best model (m4)

Term	Estimate	SE	*df*	*t* value	*p* value
(Intercept)	−10.031	0.188	345.2	−53.35	$< 2\times10^{-16}$ ***
ln D	3.729	0.057	356	65.62	$< 2\times10^{-16}$ ***
N 112	−0.930	0.252	356.1	−3.70	0.00025 ***
N 224	−1.069	0.259	356	−4.13	4.6×10^{-5} ***
N 336	−0.879	0.256	356.1	−3.43	0.00067 ***
Density	0.077	0.004	356.1	17.92	$< 2\times10^{-16}$ ***
ln D × N 112	0.262	0.077	356.1	3.4	0.00076 ***
ln D × N 224	0.293	0.079	356	3.7	0.00025 ***
ln D × N 336	0.232	0.078	356.1	2.99	0.00297 **

314 Note: Estimates are on the natural-log scale. N112, N224, N336 refer to nitrogen rates of 112, 224, 336 kg N·ha^{-1}, respectively; the reference level is 0 kg N·ha^{-1}. *df* = Satterthwaite denominator degrees of freedom. Significance codes: *** $p < 0.001$; ** $p < 0.01$; * $p < 0.05$.

318 **Table 6** Morphological lodging resistance index (MLRI = D^4/H^2) across four nitrogen rates.

Nitrogen rate (kg N·ha^{-1})	*n*	MLRI mean	SD	SE
0	93	8.63	3.99	0.414
112	93	8.75	4.22	0.437
224	93	9.12	3.93	0.407
336	91	11.67	5.43	0.569

320 Note: Values are means ± SD; SE = standard error.

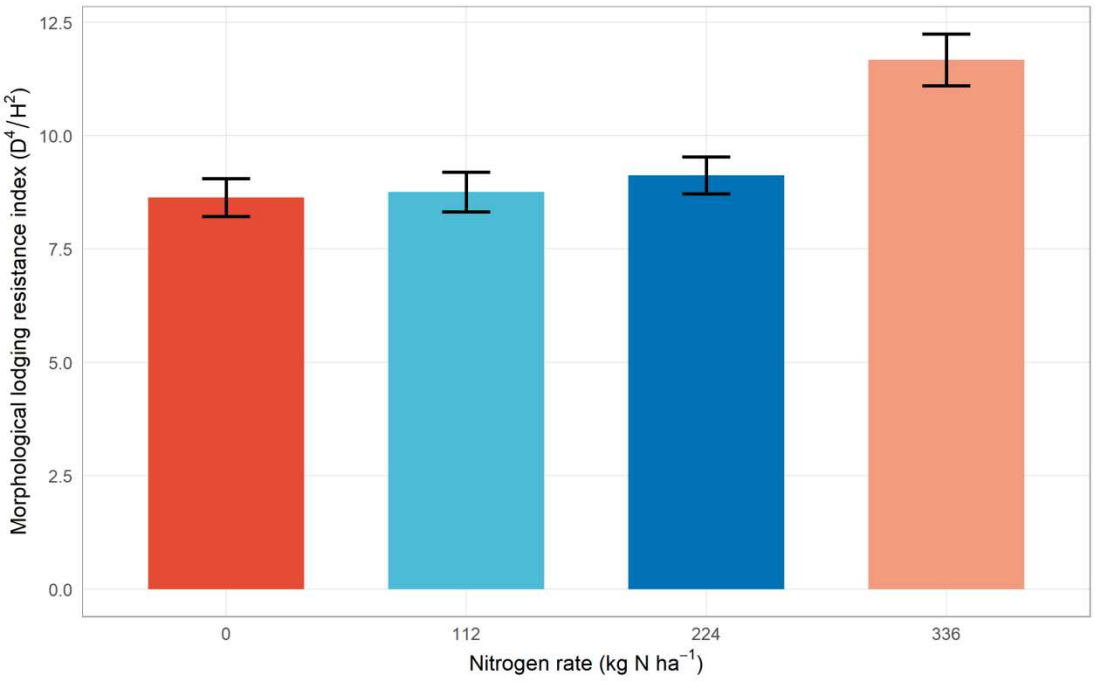


Figure 1. Morphological lodging resistance index (MLRI = D^4/H^2) across four nitrogen rates (0, 112, 224, 336 kg N·ha^{-1}). Bars represent means; error bars show 1 SE. Sample sizes: n = 93, 93, 93, 91.

3.3 Two-pathway effects of plant density

Plant density showed contrasting patterns across analytical levels. Group means declined monotonically from Low (12.4 ± 4.9, n = 105) to Medium (10.4 ± 4.2, n = 76) to High (7.6 ± 3.5, n = 189) (Table 7, Figure 2), representing a 39% reduction from low to high density. The reduction was not uniform across density classes: the drop from Low to Medium was 2.0 MLRI units (a 16% decrease), whereas the drop from Medium to High was 2.8 MLRI units (a 27% decrease), suggesting that density effects on MLRI intensify at the upper end of the density range.

In contrast, the partial coefficient for standardized density in the best model was strongly positive (β = +0.077, SE = 0.004, $p < 2\times10^{-16}$). After controlling for stem diameter and nitrogen, higher density was associated with higher MLRI, a direct effect opposite in sign to the group mean trend. The effect size is substantial: a one-standard-deviation increase in density (equivalent to approximately 3.1 plants·m^{-2} in this dataset) was associated with a 7.7% increase in MLRI at a fixed stem diameter.

The apparent paradox resolves into two independent pathways acting on the

allometric basis of lodging resistance: (1) Indirect pathway: high density → reduced stem diameter → lower MLRI; (2) Direct pathway: high density → suppressed plant height → higher MLRI.

The partial coefficient captures only the direct pathway, whereas group means reflect the combination of both. Density and *ln*(D) were not collinear ($GVIF_{adj}^{\left(\frac{1}{2df}\right)}$ = 1.283 and 1.351, respectively; Table 8), with all predictors below the 1.5 threshold, supporting the statistical separability of the two pathways. VIF values are visualized in Figure S3.

Table 7 Morphological lodging resistance index (MLRI = D^4/H^2) across three plant density classes.

Density class	Range (plants·m^{-2})	*n*	MLRI mean	SD	SE
Low	< 7	105	12.4	4.92	0.48
Medium	7–9	76	10.37	4.22	0.484
High	> 9	189	7.6	3.47	0.252

Note: Values are means ± SD; SE = standard error. Density classes: Low (< 7 plants·m^{-2}), Medium (7–9 plants·m^{-2}), High (> 9 plants·m^{-2}).

Table 8 Generalized variance inflation factors (VIF) for predictors in the mixed-effects model.

Predictor	GVIF	*df*	$GVIF_{adj}^{\left(\frac{1}{2df}\right)}$	Status
ln(D)	1.826	1	1.351	No collinearity
N rate	1.195	3	1.03	No collinearity
Density	1.646	1	1.283	No collinearity

Note: $GVIF_{adj}^{\left(\frac{1}{2df}\right)}$ accounts for the degrees of freedom of multi-level factors. Values < 1.5 indicate no collinearity. *df* = degrees of freedom.

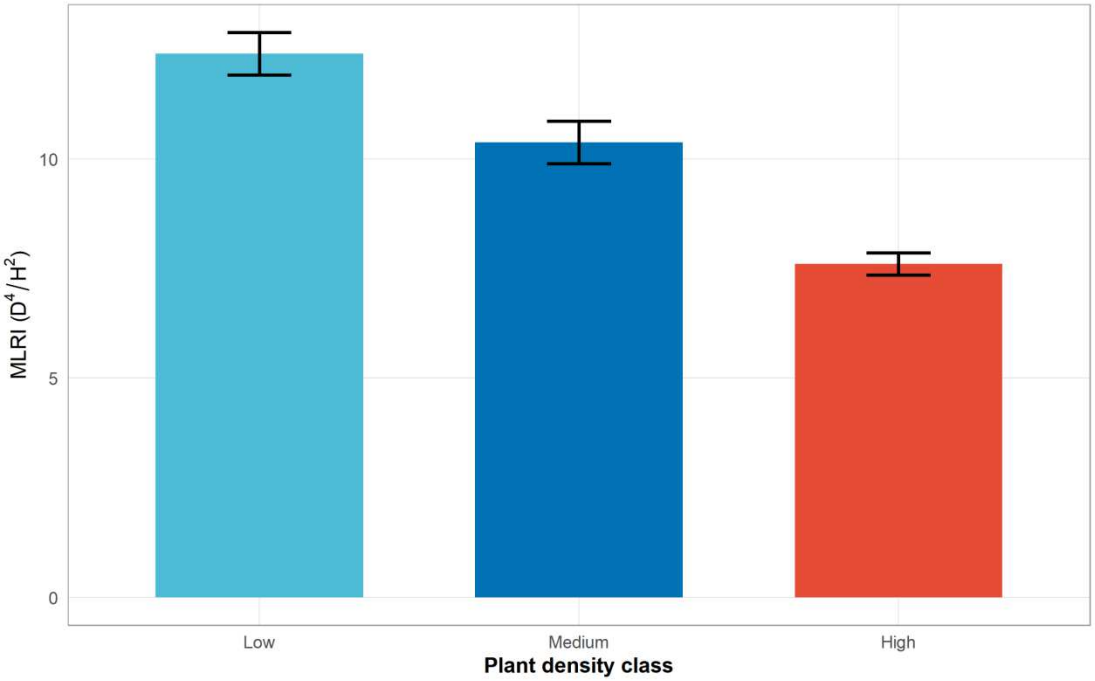


Figure 2. Morphological lodging resistance index (MLRI = D^4/H^2) across three plant density classes (Low: < 7 plants·m^{-2}, *n* = 105; Medium: 7–9 plants·m^{-2}, *n* = 76; High: > 9 plants·m^{-2}, *n* = 189). Bars: means; error bars: 1 SE.

3.4 Hybrid-specific allometric strategies

The hybrid random intercept variance was 0.0082 and residual variance 0.0040, giving an ICC of 0.671 (Table 9). Hybrid identity accounted for 67% of the unexplained variance in *ln*(MLRI), a substantially larger proportion than typical genotype-by-environment trials for morphological traits.

Hybrid marginal means ranged from 2.009 (P1442YHRCE) to 2.252 (P1366YHRCC) on the natural-log scale (Table 10), corresponding to a 27% difference on the original MLRI scale.When expressed as deviations from the grand mean, four of six hybrids differed significantly from zero: P1366YHRCC (+0.103), P1213YHR (+0.075), and P1093Q (+0.022) were significantly above the mean, whereas P1108Q (−0.070) and P1442YHRCE (−0.139) were significantly below; only P0825AM (+0.009, $p = 0.205$) did not differ from the mean (Figure 3). Pairwise comparisons revealed that 13 of 15 hybrid pairs differed significantly ($p < 0.001$; Table S1). The two non-significant pairs were P0825AM *vs*. P1093Q ($p = 0.880$) and P1213YHR *vs*. P1366YHRCC ($p = 0.158$). Hybrid BLUP values are provided in Table S2, and mean

MLRI values for each hybrid × nitrogen combination are provided in Table S3. Simple effects of hybrid within each nitrogen level are provided in Table S4.

The heatmap of MLRI across hybrid × nitrogen combinations (Figure 4) showed that hybrid rankings were largely consistent across nitrogen levels. P1366YHRCC maintained the highest MLRI at every nitrogen level (10.2–14.7), whereas P1442YHRCE consistently showed the lowest values (5.9–9.2). The divergence between these extremes was largest at 336 kg N·ha^{-1} (14.7 *vs*. 9.2, a difference of 5.5 MLRI units), suggesting that high-nitrogen environments were particularly informative for discriminating allometric strategies among genotypes. Hybrid differences within each nitrogen level showed no evidence of rank reversals.

Table 9 Variance components and intraclass correlation coefficient (ICC) for hybrid identity.

Component	Variance	ICC
Hybrid (random intercept)	0.0082	—
Residual	0.004	—
ICC	—	0.671

Note:$ICC = \sigma^2_{hybrid} / (\sigma^2_{hybrid} + \sigma^2_{residual})$. The ICC represents the proportion of unexplained variance attributable to hybrid identity.

Table 10 Hybrid marginal means of ln(MLRI) and contrasts against the grand mean.

Hybrid	emmean	SE	95% CI	Deviation	*p* value
P1366YHRCC	2.252	0.0082	(2.235, 2.268)	0.103	< 0.0001
P1213YHR	2.224	0.0083	(2.208, 2.240)	0.075	< 0.0001
P1093Q	2.171	0.0082	(2.154, 2.187)	0.022	0.0039
P0825AM	2.158	0.0081	(2.142, 2.174)	0.009	0.205
P1108Q	2.079	0.0082	(2.063, 2.095)	−0.070	< 0.0001
P1442YHRCE	2.009	0.008	(1.993, 2.025)	−0.139	< 0.0001

Note: Marginal means were obtained from a fixed-effects version of the best-fitting model. Deviation = contrast of each hybrid against the grand mean (FDR-adjusted). Values are on the natural-log scale. Hybrids are ordered by decreasing marginal mean. Tukey-adjusted pairwise comparisons are provided in Table S1.

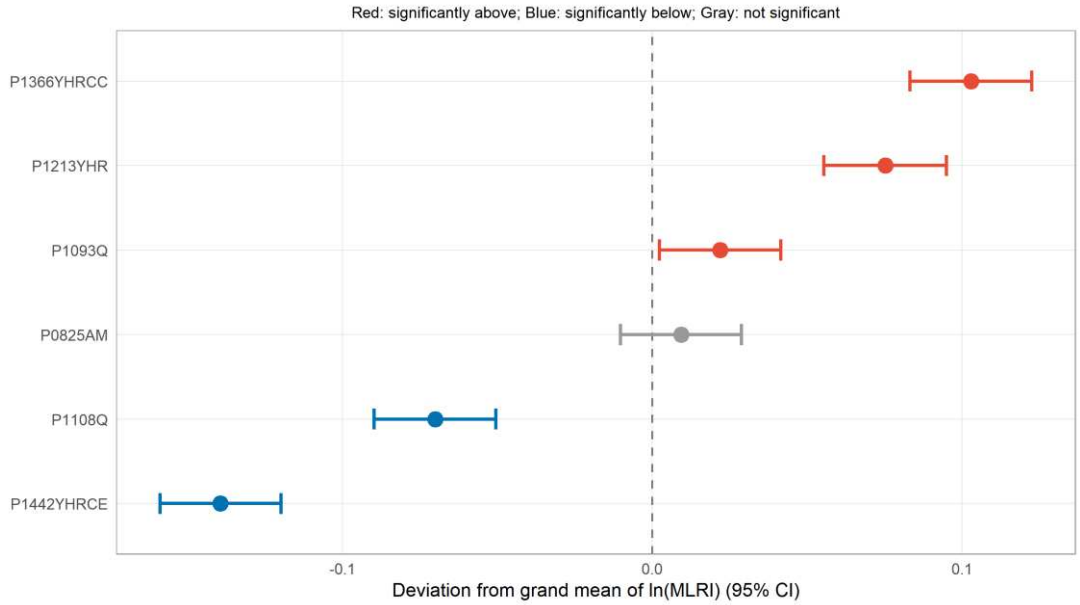


Figure 3 Hybrid deviations from the grand mean of *ln*(MLRI) with 95% confidence intervals. Red: significantly above the grand mean; blue: significantly below; gray: not significantly different. Estimates are on the natural-log scale. n = 370 observations across six hybrids.

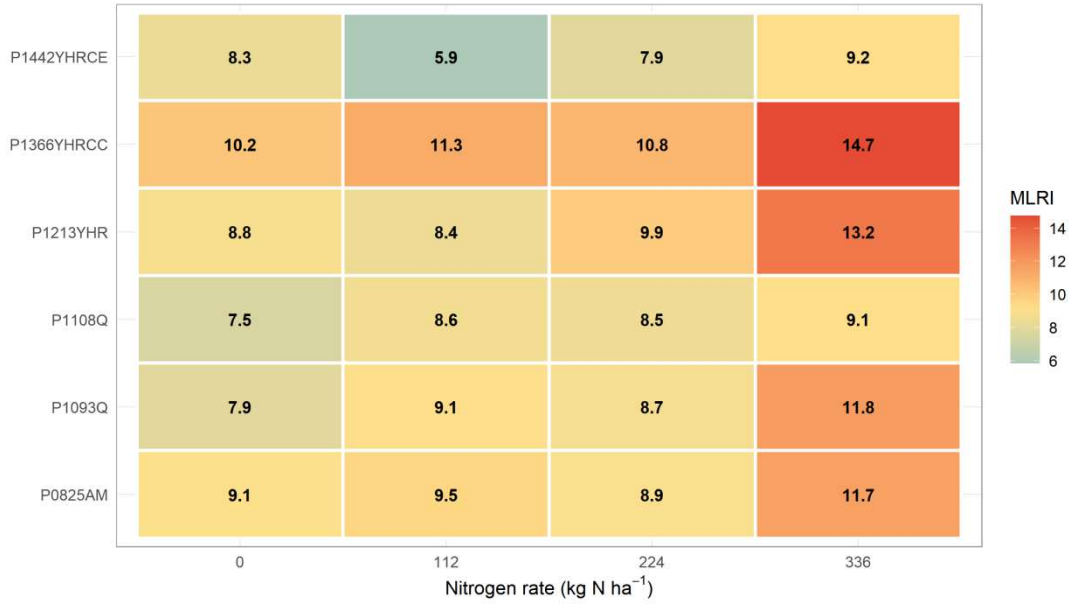


Figure 4 Heatmap of MLRI across hybrid × nitrogen combinations. Nitrogen rates on the x-axis are shown in metric units (0, 112, 224, 336 kg N·ha^{-1}). Numbers in each cell indicate mean MLRI. Red: high lodging resistance; blue: low.

3.5 Robustness and model diagnostics

Three MLRI formulations were nearly identical in rank order (Table 11): Spearman ρ = 0.9942 for D^4/H^2 *vs*. D^3/H, ρ = 1.0000 for D^4/H^2 *vs*. D^2/H, and ρ = 0.9942

for D^3/H *vs*. D^2/H (all $p < 2.2\times10^{-16}$). The near-unity correlation between D^4/H^2 and D^2/H reflects the fact that stem diameter dominates MLRI variance in this dataset ($r^2 > 0.91$ between *ln*(D) and *ln*(MLRI)), so the choice of exponent has only a marginal effect on treatment and genotype rankings.

Mixed-effects models fitted to each formulation produced qualitatively identical coefficients (Table 12). The *ln*(D) × N300 interaction was significant under all three formulations (+0.232, +0.116, +0.116; all $p < 0.01$), as was the density effect (+0.077, +0.038, +0.038; all $p < 2\times10^{-16}$). Marginal R^2 ranged from 0.939 to 0.974, and conditional R^2 from 0.980 to 0.992 (Table S5) . The rank order of hybrid effects was also preserved: P1366YHRCC remained highest and P1442YHRCE lowest under all three formulations. These results confirm that the main conclusions of this study are not artifacts of the specific exponent chosen for MLRI. A visual comparison of coefficients across formulations is provided in Figure S4, and hybrid BLUP values are shown in Figure S5.

Residual diagnostics (Table 13, Figure 5) revealed mild non-normality (Shapiro-Wilk W = 0.9858, $p = 0.0011$) and heteroscedasticity (Breusch-Pagan BP = 45.09, $df = 8$, $p = 3.5\times10^{-7}$). Residuals showed no systematic patterns across fitted values, *ln*(D), or the Q-Q plot. The mild departures from ideal diagnostic assumptions are common in large field phenotyping datasets with $n > 300$ and do not invalidate coefficient inference given the large sample size ($n = 370$). Cross-validation performance ($R^2 = 0.923$, RMSE = 0.126; Table 4) closely matched the model's marginal R^2 (0.946), indicating no substantial overfitting.

Table 11. Spearman rank correlations among three morphological lodging resistance index formulations.

Pair	Spearman ρ	p value
D^4/H^2 *vs* D^3/H	0.9942	$< 2.2\times10^{-16}$
D^4/H^2 *vs* D^2/H	1.0000	$< 2.2\times10^{-16}$
D^3/H *vs* D^2/H	0.9942	$< 2.2\times10^{-16}$

Note: All correlations were computed on 370 observations.

Table 12. Sensitivity analysis of key model coefficients across three MLRI formulations.

MLRI form	Term	Estimate	SE	*p* value
D^4/H^2	ln D	3.729	0.057	$< 2\times10^{-16}$
D^4/H^2	N 112	−0.930	0.252	0.00025
D^4/H^2	N 336	−0.879	0.256	0.00067
D^4/H^2	Density	0.077	0.004	$< 2\times10^{-16}$
D^4/H^2	ln D × N336	0.232	0.078	0.003
D^3/H	ln D	2.864	0.028	$< 2\times10^{-16}$
D^3/H	N 112	−0.465	0.126	0.00025
D^3/H	N 336	−0.439	0.128	0.00067
D^3/H	Density	0.038	0.002	$< 2\times10^{-16}$
D^3/H	ln D × N336	0.116	0.039	0.003
D^2/H	ln D	1.864	0.028	$< 2\times10^{-16}$
D^2/H	N 112	−0.465	0.126	0.00025
D^2/H	N 336	−0.439	0.128	0.00067
D^2/H	Density	0.038	0.002	$< 2\times10^{-16}$
D^2/H	ln D × N336	0.116	0.039	0.003

Note: Estimates are on the natural-log scale. All models include a random intercept for hybrid. The reference level for nitrogen is 0 kg N·ha^{-1}. N112, N224, N336 refer to nitrogen rates of 112, 224, 336 kg N·ha-1, respectively.

Table 13 Residual diagnostics for the best-fitting model (m4).

Test	Statistic	*df*	*p* value	Conclusion
Shapiro-Wilk (normality)	W = 0.9858	—	0.0011	Mild non-normality
Breusch-Pagan (homoscedasticity)	BP = 45.09	8	3.54×10^{-7}	Heteroscedastic

Note: Shapiro-Wilk tests the null hypothesis that residuals are normally distributed. Breusch-Pagan tests the null hypothesis of homoscedasticity. With n = 370 and Satterthwaite approximation, coefficient inference remains robust to these mild departures.

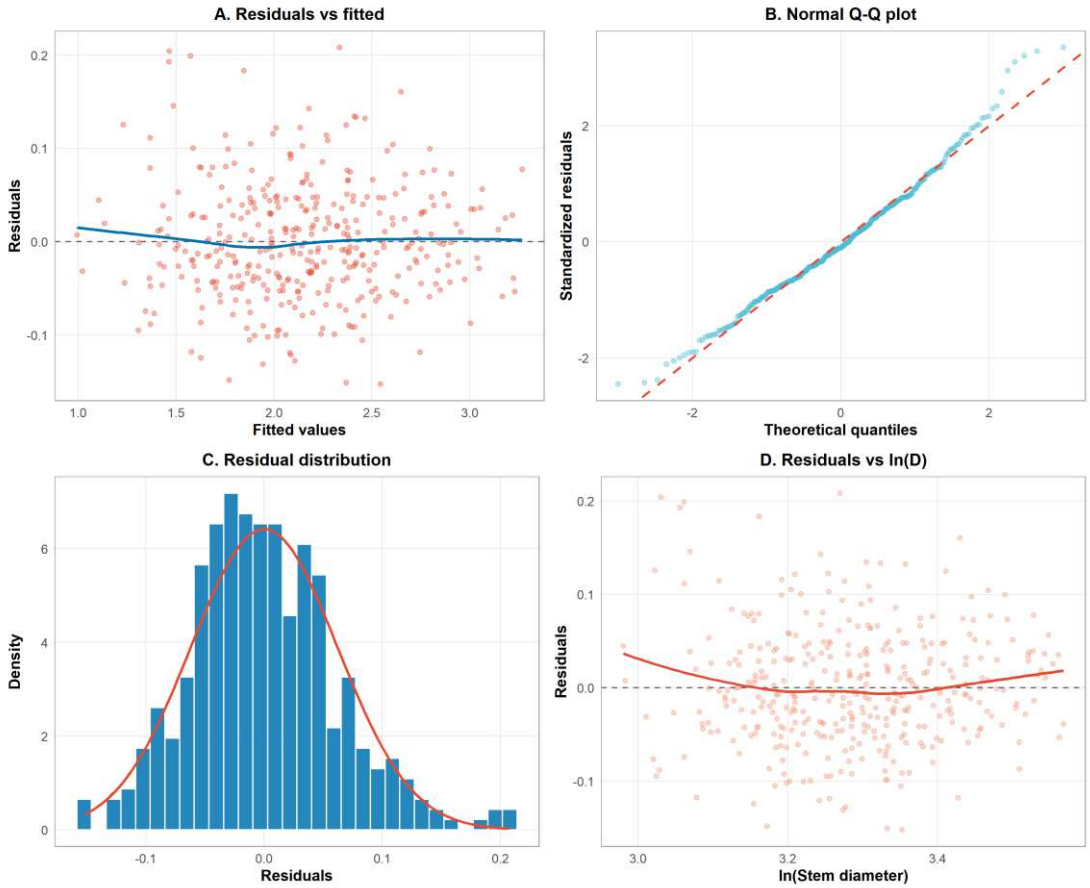


Figure 5 Residual diagnostics of the best-fitting mixed-effects model (m4). (A) Residuals versus fitted values with a LOESS smoother; (B) normal Q-Q plot of standardized residuals; (C) histogram of residuals with normal density overlay; (D) residuals versus ln(stem diameter). The model showed mild non-normality (Shapiro-Wilk W = 0.9858, $p = 0.0011$) and heteroscedasticity (Breusch-Pagan BP = 45.09, $df = 8$, $p = 3.5\times10^{-7}$), which are common in large field phenotyping datasets and do not invalidate coefficient inference given the sample size ($n = 370$).

4 Discussion

4.1 Nitrogen reshapes the allometric basis through a dual mechanism

Our results reveal that nitrogen reshapes the allometric basis of morphological lodging resistance through two opposing mechanisms. At a fixed stem diameter, higher nitrogen reduced MLRI (negative N main effect), consistent with allometric theory predicting a lower D–H scaling exponent under high resource availability [22, 23, 47]. Nitrogen-driven internode elongation increases plant height at a faster rate than stem diameter, so plants become relatively taller for a given diameter, an architectural shift

that reduces mechanical stability.

However, nitrogen also increased stem diameter by an average of 2.8 mm from 0 to 336 kg N·ha^{-1}, and this increase dominated the net effect through the D^4 term. The result was a 35% net increase in MLRI across the nitrogen gradient. This finding reconciles two seemingly contradictory observations in the literature: that high nitrogen promotes stem thickness (positive effect on lodging resistance) yet is often associated with increased lodging incidence in the field (negative effect) [21,23]. The resolution is that MLRI responds to the allometric balance between D and H, not to either trait alone.

This has practical implications for breeding and agronomy. Simple recommendations to "increase nitrogen for stronger stems" are incomplete: high nitrogen can reduce lodging resistance in plants with already-large stem diameters, while smaller-diameter varieties may benefit more from nitrogen-driven thickening. Future work should test whether the observed allometric trade-off can be decoupled through genetic selection targeting the D–H scaling exponent [31], or through chemical regulation of allometric trait behavior [48].

4.2 Density reshapes the allometric basis through two independent pathways

Plant density showed opposite patterns in simple and partial analyses. This is not a contradiction but the expected consequence of two independent pathways acting on the allometric basis of lodging resistance. High density reduces stem diameter (lowering MLRI) and suppresses plant height (raising MLRI). The net effect on simple means reflects the relative magnitude of both pathways; the partial coefficient isolates the direct effect of density on MLRI via plant height.

That density remained significant even after controlling for stem diameter and nitrogen indicates that plant height plasticity is an independent contributor to morphological lodging resistance. This is consistent with agronomic observations that dense canopies produce shorter, more compact plants, an architectural response that partially offsets the mechanical penalty of thinner stems [5,25]. Breeding programs targeting high-density tolerance should therefore evaluate MLRI under realistic dense-canopy conditions, not under low-density spacing.

The statistical separability of the two density pathways, confirmed by VIF analysis (all $GVIF_{adj}^{\left(\frac{1}{2df}\right)} < 1.5$), supports an interpretation in which density acts as a canopy-level architectural signal rather than as a simple stressor. This distinction could be incorporated into canopy-level lodging risk models by treating density as an architectural modifier rather than a stress factor. This distinction may be useful for modeling canopy-level lodging risk in dense production systems [20].

4.3 Hybrid-specific allometric strategies and breeding implications

Hybrid identity explained 67% of the unexplained variance in ln(MLRI), and 13 of 15 pairwise comparisons were significant. The magnitude of these differences (0.243 ln units between P1366YHRCC and P1442YHRCE, equivalent to a 27% difference in MLRI) is agronomically meaningful and suggests that selection for morphological lodging resistance is feasible within existing commercial germplasm [26].

The consistent ranking across nitrogen levels, with P1366YHRCC always highest and P1442YHRCE always lowest, indicates that genetic differences in the allometric basis of lodging resistance are stable across environments. This stability makes MLRI an attractive selection criterion for breeding programs, especially when combined with robot phenotyping for high-throughput field evaluation [17]. The divergence between the two extreme hybrids was largest at 336 kg N·ha^{-1} (14.7 *vs*. 9.2), suggesting that high-nitrogen environments are particularly informative for discriminating allometric strategies among genotypes.

4.4 Methodological contributions and limitations

This study demonstrates several methodological contributions relevant to morphological phenotyping. Mixed-effects modeling properly separates genotype from fixed treatment effects and enables variance partitioning through the ICC [40]. Common-sample fitting ensures comparability of AIC and BIC across candidate models [37]. Robustness checks across three MLRI formulations confirm that results are not driven by the specific exponent. Finally, estimated marginal means with Tukey adjustment provide reliable hybrid comparisons even with only six genotypes, avoiding the overly wide bootstrap confidence intervals that arise when random-effect variances

are estimated from a small number of levels [39].

Several limitations should be acknowledged. First, all data come from a single site-year, limiting generalization; multi-environment validation is needed before the specific hybrid rankings can be extended to other production environments. Second, MLRI = D^4/H^2 is theoretically grounded but does not capture stem tissue mechanical properties such as rind thickness or elastic modulus; mechanical validation on a subset of genotypes is a necessary next step [10, 11,19]. Third, stem diameter alone does not guarantee lodging resistance in the field: thick-stemmed plants can still lodge if they are tall, have thin stem walls, low lignin or cellulose content, poor root anchorage, or high wind exposure. MLRI is therefore a morphological proxy for lodging resistance potential, not a direct measure of actual lodging resistance. It should be used to prioritize genotypes for subsequent mechanical testing, anatomical characterization, and field-based lodging assessment, rather than as a stand-alone selection criterion. Fourth, the dataset contains only morphological traits, and future studies should link MLRI to actual grain yield and lodging incidence under natural or artificial lodging conditions. Fifth, residual diagnostics showed mild non-normality and heteroscedasticity, though with n = 370 and the Satterthwaite approximation, coefficient inference remains robust.

4.5 Implications for high-throughput phenotyping

The strong fit of the model (marginal R^2 = 0.946) and the robustness of MLRI across formulations (Spearman $\rho \geq 0.994$) support the use of D^4/H^2 as a high-throughput proxy for lodging resistance screening. Unlike mechanical phenotyping, which requires destructive sampling of individual stalks, MLRI can be computed from the same robot-derived D and H measurements that are already collected in many breeding programs [17,19]. This makes MLRI a cost-effective addition to existing phenotyping pipelines, particularly for early-generation selection where destructive sampling is impractical.

5 Conclusion

Lodging remains a major constraint to maize productivity worldwide, and understanding how agronomic practices reshape the morphological basis of lodging resistance is essential for both breeding and crop management. This work provides a

quantitative framework for that question by combining robot-phenotyping data with mixed-effects models. The results indicate that stem diameter remains the dominant driver of the morphological lodging resistance index (MLRI = D^4/H^2), but nitrogen and density each act through two opposing pathways. Nitrogen reduces MLRI at a fixed stem diameter yet increases it indirectly by promoting stem thickening, producing a net 35% gain across the nitrogen gradient. Density reduces stem diameter (lowering MLRI) but also suppresses plant height (raising MLRI), and these two pathways are statistically separable. Hybrid identity explains 67% of the residual variance, with stable rankings across nitrogen levels, indicating that genetic differences in D–H allometry are consistent and selectable. The index is robust across three formulations and can be derived from existing TerraSentia-based measurements of stem diameter and plant height, making it a practical morphological proxy that can be used to prioritize genotypes for subsequent mechanical and field validation. Because this study is limited to one site-year and morphological traits, future work should validate MLRI against mechanical strength and field lodging incidence in multi-environment trials before it is widely adopted in breeding programs.

Declarations

Ethics approval and consent to participate

Not applicable.

Consent for publication

Not applicable.

Competing interests

The authors declare no conflict of interest.

Funding

The work was supported by the Doctoral Research Start-up Fund of Henan Agricultural University (Grant No. 30500975), the Doctoral Research Startup Project of Wenzhou Vocational College of Science and Technology (No: 2406), and Key Project for Industrial Upgrading in Longwan Modern Agricultural Industry Research Institute (No: 2025LWYJY20).

Authors' Contributions

Conceptualization, M.Z., and J.S.; Methodology, M.Z.,C.B., and J.S.; Formal Analysis, C.B., N.Z.,and F.G.; Writing – Original Draft, M.Z., C.B., and J.S.; Writing – Review & Editing, M.Z., C.B., D.Y., S. Y., and J.S.; Supervision, M.Z. and J.S.. All authors have read and approved the final manuscript.

Acknowledgments

We are grateful to Wenxue Li (Institute of Crop Sciences, Chinese Academy of Agricultural Sciences) and Pengshuai Yan (College of Agronomy, Henan Agricultural University) for their constructive comments on the manuscript and helpful discussions on lodging resistance mechanisms. We also thank all people contributing to experimental materials collection and data acquisition for this study. Finally, we appreciate the editor and the anonymous reviewers for their in-depth comments, suggestions, and corrections, which have greatly improved the manuscript.

Availability of data and materials

The original dataset analyzed in this study is publicly available from the Dryad Digital Repository at https://doi.org/10.5061/dryad.bnzs7h4f1. Analysis scripts are available from the corresponding author upon reasonable request. For collaboration inquiries or questions regarding the analysis, please contact the corresponding author.

References

[1] Shah, A.N., Tanveer, M., Abbas, A., Yıldırım, M., Shah, A.A., Ahmad, M.I., Wang, Z.W., Sun, W.W., Song, Y.H., 2021. Combating dual challenges in maize under high planting density: Stem lodging and kernel abortion. Front. Plant Sci. 12, 699085.

[2] Sher, A., Iqbal, J., Nazeer, W., Maqbool, M.M., Nadeem, M., Faiz, S., Khan, S., 2022. A review on overcoming dual challenges for maize cropping under high plant density: Stalk lodging and kernel abortion. J. Bioresour. Manag. 9, 56–74.

[3] Berry, P.M., Sterling, M., Spink, J.H., Baker, C.J., Sylvester-Bradley, R., Mooney, S.J., Tams, A.R., Ennos, A.R., 2004. Understanding and reducing lodging in cereals. Adv. Agron. 84, 217–271.

[4] Novacek, M.J., Mason, S.C., Galusha, T.D., Yaseen, M., 2013. Twin rows minimally impact irrigated maize yield, morphology, and lodging. Agron. J. 105, 268–276.

[5] Xue, J., Xie, R.Z., Zhang, W.F., Wang, K.R., Hou, P., Ming, B., Gou, L., Li, S.K., 2017. Research progress on reduced lodging of high-yield and -density maize. J. Integr. Agric. 16, 2717–2725.

[6] Mengistie, E., McDonald, A.G., 2023. Effect of cell wall compositions on lodging resistance of cereal crops: Review. J. Agric. Sci. 161, 794–807.

[7] Yang, L., Liu, J., Li, N., Pei, Y., Peng, J., Wang, Z., 2023. An integrated strategy coordinating endogenous and exogenous approaches to alleviate crop lodging. Plant Stress 9, 100197.

[8] Kong, E., Liu, D., Guo, X., Yang, W., Sun, J., Li, X., Zhan, K., Cui, D., Lin, J., Zhang, A., 2013. Anatomical and chemical characteristics associated with lodging resistance in wheat. Crop J. 1, 43–49.

[9] Pellerin, S., Trend, M., Doré, T., 1990. Effect of mutual shading on the emergence of nodal roots and the root/shoot ratio of maize. Plant Soil 125, 21–29.

[10] Stubbs, C.J., McMahan, C.S., Tabaracci, K., Schnable, P.S., 2023. Unveiling the phenotypic landscape of stalk lodging resistance in diverse maize hybrids. Field Crops Res. 304, 109168.

[11] Tabaracci, K., Bokros, N.T., Oduntan, Y., Kunduru, B., DeKold, J., Mengistie, E., McDonald, A.G., Stubbs, C.J., Sekhon, R.S., DeBolt, S., Robertson, D.J., 2024. Biomechanical phenotyping pipeline for stalk lodging resistance in maize. MethodsX 12, 102562.

[12] Navabi, A., Iqbal, M., Strenzke, K., Spaner, D., 2006. The relationship between lodging and plant height in a diverse wheat population. Can. J. Plant Sci. 86, 723–726.

[13] Ookawa, T., Hobo, T., Yano, M., Murata, K., Ando, T., Miura, H., Asano, K., Ochiai, Y., Ikeda, M., Nishitani, R., Ebitani, T., Ozaki, H., Angeles, E.R., Hirasawa, T., Matsuoka, M., 2010. New approach for rice improvement using a pleiotropic QTL gene for lodging resistance and yield. Nat. Commun. 1, 132.

[14] Niklas, K.J., 1999. The influence of gravity and wind on land plant evolution. Rev. Palaeobot. Palynol. 102, 1–14.

[15] Song, Y., Birch, C., Luquet, D., Hanan, J., 2012. Allometric relationships of canopy

635 organ development in rice and maize, in: Proceedings of the 16th Australian
636 Agronomy Conference, pp. 1–4.
637 [16] Spatz, H.C., Bruechert, F., 2000. Basic biomechanics of self-supporting plants:
638 Wind loads and gravitational loads on a Norway spruce tree. For. Ecol. Manag.
639 135, 33–44.
640 [17] DeBruin, J., Aref, T., Tirado Tolosa, S., Hensley, R., Underwood, H., McGuire, M.,
641 Soman, C., Nystrom, G., Parkinson, E., Li, C., Moose, S.P., Chowdhary, G., 2025.
642 Breaking the field phenotyping bottleneck in maize with autonomous robots.
643 Commun. Biol. 8, 467.
644 [18] Kunduru, B., Bokros, N.T., Tabaracci, K., Kumar, R., Brar, M.S., Stubbs, C.J.,
645 Oduntan, Y., DeKold, J., Bishop, R., Woomer, J., Verges, V., McDonald, A.G.,
646 McMahan, C.S., DeBolt, S., Robertson, D.J., Sekhon, R.S., 2025. High-density
647 phenotype data of intermediate phenotypes associated with stalk lodging
648 resistance in maize. Sci. Data 12, 1721.
649 [19] Ma, D., Xie, R., Yu, X., Li, S., Gao, J., 2024. Historical trends in maize morphology
650 from the 1950s to the 2010s in China. Field Crops Res. 306, 109210.
651 [20] Liu, X., Meng, Y., Dong, L., Hao, Y., Yu, Y., Lv, G., Jiang, Y., Zhang, Y., Qian, C.,
652 Gu, W., 2026. Synergistic modulation of nitrogen and chemical regulation:
653 Balancing photosynthesis and lodging resistance for high-efficiency maize
654 production under dense planting. Plants 15, 500.
655 [21] Shi, D.Y., Li, Y.H., Zhang, J.W., Liu, P., Zhao, B., Dong, S.T., 2024. Effects of
656 plant density and nitrogen rate on lodging-related stalk traits of summer maize.
657 Plant Soil Environ. 70, 89–99.
658 [22] Sun, S., Zhang, X., Wang, Y., Wang, Y., Wang, Z., 2020. Optimizing nitrogen
659 fertilization for lodging resistance in maize: A review. Field Crops Res. 246,
660 107662.
661 [23] Zhai, J., Ming, B., Zhang, G., Zhang, Y.-m., Cao, Y., Xie, R., Wang, K., Li, S., Xue,
662 J., Gou, L., 2025. Nitrogen rate, density, and plant architecture jointly determine
663 lodging risk in drip fertigated spring maize. Ann. Agric. Sci. 70, 100399.
664 [24] Kong, F., Liu, F., Li, X., Yin, P., Lan, T., Feng, D., Song, B., Lei, E., Li, Z., Wang,

X., Yuan, J., 2024. Ecological factors regulate stalk lodging within dense planting maize. Field Crops Res. 317, 109529.

[25] Mansfield, B.D., Mumm, R.H., 2014. Survey of plant density tolerance in U.S. maize germplasm. Crop Sci. 54, 157–173.

[26] Yue, H., Olivoto, T., Bu, J., Wei, J., Liu, P., Wu, W., Nardino, M., Jiang, X., 2025. Assessing the role of genotype by environment interaction as determinants of maize grain yield and lodging resistance. BMC Plant Biol. 25, 120.

[27] Huang, J., Yang, Y., Zhou, F., Deng, X., 2023. Biomechanical stability variation of rice stem during maturation and wilting. J. Braz. Soc. Mech. Sci. Eng. 45, 74.

[28] Qi, B., Hu, J., Zhu, L., Duan, Y., Zhang, W., Gou, L., 2023. Response of maize stalk to plant density on cellulose accumulation by modulating enzymes activities. Field Crops Res. 304, 109152.

[29] Chen, P., Zhao, L., Zhang, Z.-L., Song, L.-Z., Zhao, X.-F., Zhang, X., Duan, X.-R., Liang, M., Zhang, C., Wang, C.-Y., 2026. The effect of the interaction of nitrogen fertilization with planting density on maize (Zea mays L.) yield, stalk mechanical properties, and enzyme activity. Plants 15, 459.

[30] Liu, F., Zhou, F., Wang, X., Zhan, X., Guo, Z., Liu, Q., Wei, G., Lan, T., Feng, D., Kong, F., Yuan, J., 2023. Enhancing the basal internode mechanical strength by improving the canopy light distribution of dense planting maize to reduce the lodging rate. Eur. J. Agron. 148, 126871.

[31] Wang, Q., Xue, J., Zhang, G., Chen, J., Xie, R., Ming, B., Hou, P., Wang, K., Li, S., 2024. Nitrogen split application can improve the stalk lodging resistance of maize planted at high density. Agronomy 14, 985.

[32] Bates, D., Mächler, M., Bolker, B., Walker, S., 2015. Fitting linear mixed-effects models using lme4. J. Stat. Softw. 67, 1–48.

[33] R Core Team, 2024. R: A Language and Environment for Statistical Computing. R Foundation for Statistical Computing, Vienna, Austria.

[34] Bolker, B.M., Brooks, M.E., Clark, C.J., Geange, S.W., Poulsen, J.R., Stevens, M.H.H., White, J.S.S., 2009. Generalized linear mixed models: A practical guide for ecology and evolution. Trends Ecol. Evol. 24, 127–135.

695 [35] Zuur, A.F., Ieno, E.N., Walker, N.J., Saveliev, A.A., Smith, G.M., 2009. Mixed
696 Effects Models and Extensions in Ecology with R. Springer, New York.
697 [36] Akaike, H., 1974. A new look at the statistical model identification. IEEE Trans.
698 Autom. Control 19, 716–723.
699 [37] Burnham, K.P., Anderson, D.R., 2002. Model Selection and Multimodel Inference:
700 A Practical Information-Theoretic Approach, 2nd ed. Springer, New York.
701 [38] Lenth, R.V., 2024. emmeans: Estimated Marginal Means, aka Least-Squares
702 Means. R package version 1.10.1.
703 [39] Tukey, J.W., 1949. Comparing individual means in the analysis of variance.
704 Biometrics 5, 99–114.
705 [40] Nakagawa, S., Schielzeth, H., 2013. A general and simple method for obtaining R^2
706 from generalized linear mixed-effects models. Methods Ecol. Evol. 4, 133–142.
707 [41] Benjamini, Y., Hochberg, Y., 1995. Controlling the false discovery rate: A practical
708 and powerful approach to multiple testing. J. R. Stat. Soc. Ser. B 57, 289–300.
709 [42] Fox, J., Weisberg, S., 2019. An R Companion to Applied Regression, 3rd ed. Sage,
710 Thousand Oaks, CA.
711 [43] Fox, J., Monette, G., 1992. Generalized collinearity diagnostics. J. Am. Stat. Assoc.
712 87, 178–183.
713 [44] Shapiro, S.S., Wilk, M.B., 1965. An analysis of variance test for normality
714 (complete samples). Biometrika 52, 591–611.
715 [45] Breusch, T.S., Pagan, A.R., 1979. A simple test for heteroscedasticity and random
716 coefficient variation. Econometrica 47, 1287–1294.
717 [46] Stone, M., 1974. Cross-validatory choice and assessment of statistical predictions.
718 J. R. Stat. Soc. Ser. B 36, 111–133.
719 [47] Weiner, J., 2004. Allocation, plasticity and allometry in plants. Perspect. Plant Ecol.
720 Evol. Syst. 6, 207–215.
721 [48] Urfan, M., Hakla, H.R., Sharma, S., Khajuria, M., Satbhai, S.B., Vyas, D., Bhougal,
722 S., Yadav, N.S., Pal, S., 2022. Paclobutrazol improves surface water use efficiency
723 by regulating allometric trait behavior in maize. Chemosphere 307, 135958.
724 [49] Zhong, S., Xu, L., Zhang, Z., Li, Y., Lin, Z., Wang, J., Huo, Q., Wang, Q., Shi, Y.,

Liu, H., Liu, J., Song, Y., Fang, X., et al., 2025. The quantitative trait locus stiff2 controls stalk bending strength and root architecture in maize. J. Genet. Genomics 53, 868–878.

Supplementary Materials

Table S1 Tukey-adjusted pairwise comparisons of hybrid marginal means of *ln*(MLRI).

Contrast	Estimate	SE	*df*	*t* ratio	*p* value
P1366YHRCC − P1442YHRCE	0.2423	0.0115	356	21.1	< 0.0001
P1213YHR − P1442YHRCE	0.2147	0.0115	356	18.74	< 0.0001
P1093Q − P1442YHRCE	0.1614	0.0114	356	14.13	< 0.0001
P0825AM − P1442YHRCE	0.1488	0.0114	356	13.06	< 0.0001
P1108Q − P1213YHR	−0.1454	0.0115	356	−12.60	< 0.0001
P0825AM − P1366YHRCC	−0.0936	0.0114	356	−8.21	< 0.0001
P1093Q − P1108Q	0.092	0.0115	356	8.02	< 0.0001
P1093Q − P1366YHRCC	−0.0810	0.0115	356	−7.06	< 0.0001
P0825AM − P1108Q	0.0794	0.0114	356	6.94	< 0.0001
P1108Q − P1442YHRCE	0.0693	0.0114	356	6.07	< 0.0001
P0825AM − P1213YHR	−0.0659	0.0115	356	−5.73	< 0.0001
P1093Q − P1213YHR	−0.0533	0.0115	356	−4.62	< 0.0001
P1213YHR − P1366YHRCC	−0.0277	0.0115	356	−2.40	0.1582
P0825AM − P1093Q	−0.0126	0.0114	356	−1.10	0.8797

Note: Values are on the natural-log scale. Tukey adjustment was applied for all 15 pairwise comparisons. Pairs are ordered by absolute effect size. Positive values indicate that the first hybrid had higher MLRI than the second.

Table S2 BLUP values of hybrid random intercepts from the mixed-effects model (m4), compared with estimated marginal mean deviations reported in Table 10.

Hybrid	BLUP (random-effects)	Deviation (fixed-effects)	Difference
P1366YHRCC	0.1021	0.103	< 0.001
P1213YHR	0.0747	0.075	< 0.001
P1093Q	0.0218	0.022	< 0.001
P0825AM	0.0093	0.009	< 0.001
P1108Q	−0.0695	−0.070	< 0.001
P1442YHRCE	−0.1383	−0.139	< 0.001

Note: BLUP from the random-effects model (m4) and deviation from the fixed-effects model differ by less than 0.001 ln units because the hybrid ICC (0.671) indicates minimal shrinkage. Both estimates are reported for transparency.

Table S3 Mean MLRI across hybrid × nitrogen combinations.

Hybrid	Nitrogen rate (kg N·ha^{-1})			
	0	112	224	336
P0825AM	9.09 (16)	9.47 (15)	8.90 (16)	11.67 (15)
P1093Q	7.88 (16)	9.14 (16)	8.73 (14)	11.81 (15)
P1108Q	7.51 (15)	8.59 (16)	8.51 (16)	9.15 (14)
P1213YHR	8.83 (14)	8.38 (15)	9.93 (16)	13.25 (15)
P1366YHRCC	10.17 (16)	11.26 (15)	10.80 (15)	14.75 (16)
P1442YHRCE	8.28 (16)	5.86 (16)	7.90 (16)	9.18 (16)

Note: Values are means of MLRI = D^4/H^2. Numbers in parentheses are the number of

plant-level observations (*n*) for each hybrid × nitrogen combination. Nitrogen rates are given in kg N·ha^{-1}.

Table S4 Simple effects of hybrid (identical across all nitrogen levels).

Contrast	Estimate	SE	df	t ratio	p value
P1366YHRCC − P1442YHRCE	0.2424	0.0115	356	21.1	< 0.0001
P1108Q − P1366YHRCC	−0.1730	0.0115	356	−15.06	< 0.0001
P1213YHR − P1442YHRCE	0.2147	0.0115	356	18.74	< 0.0001
P1093Q − P1442YHRCE	0.1614	0.0114	356	14.13	< 0.0001
P0825AM − P1442YHRCE	0.1488	0.0114	356	13.06	< 0.0001
P1108Q − P1213YHR	−0.1454	0.0115	356	−12.60	< 0.0001
P0825AM − P1366YHRCC	−0.0936	0.0114	356	−8.21	< 0.0001
P1093Q − P1108Q	0.092	0.0115	356	8.02	< 0.0001
P1093Q − P1366YHRCC	−0.0810	0.0115	356	−7.06	< 0.0001
P0825AM − P1108Q	0.0794	0.0114	356	6.94	< 0.0001
P1108Q − P1442YHRCE	0.0693	0.0114	356	6.07	< 0.0001
P0825AM − P1213YHR	−0.0659	0.0115	356	−5.73	< 0.0001
P1093Q − P1213YHR	−0.0533	0.0115	356	−4.62	< 0.0001
P1213YHR − P1366YHRCC	−0.0277	0.0115	356	−2.40	0.1582
P0825AM − P1093Q	−0.0126	0.0114	356	−1.10	0.8797

Note: Values are on the natural-log scale. Tukey adjustment was applied for all 15 pairwise comparisons. Positive estimates indicate that the first hybrid had higher MLRI than the second. Because the best-fitting model did not include a hybrid × nitrogen interaction term, comparisons were identical across all four nitrogen levels (0, 112, 224, 336 kg N·ha^{-1}) and are therefore presented once.

Table S5 Sensitivity analysis: R^2 and AIC across MLRI formulations.

MLRI form	Marginal R^2	Conditional R^2	AIC
D^4/H^2	0.939	0.98	−897.4
D^3/H	0.974	0.992	−1397.9
D^2/H	0.939	0.98	−1397.9

Note: All models included the same fixed-effects structure (*ln*(D) × N + Density) and a random intercept for hybrid. AIC = Akaike information criterion. The main conclusions (significance of *ln*(D) × N300 interaction and density effect) were preserved across all three formulations.

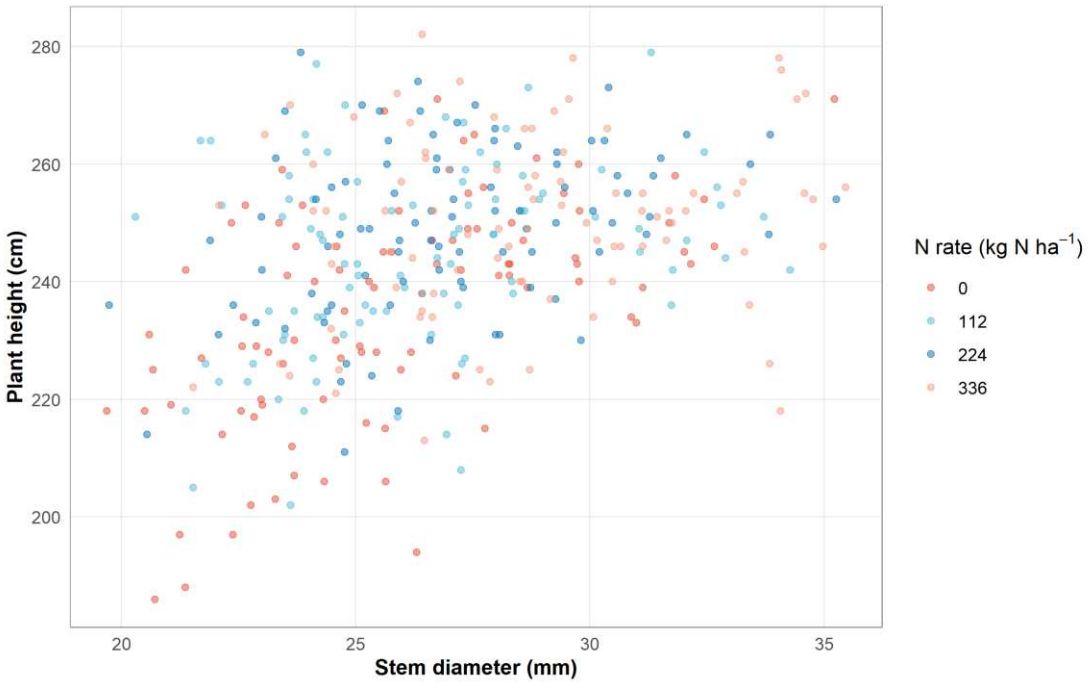


Figure S1 Joint distribution of stem diameter and plant height by nitrogen rate. Each point represents one plant-level observation (n = 370). Colors denote nitrogen rate (0, 112, 224, 336 kg N·ha^{-1}).

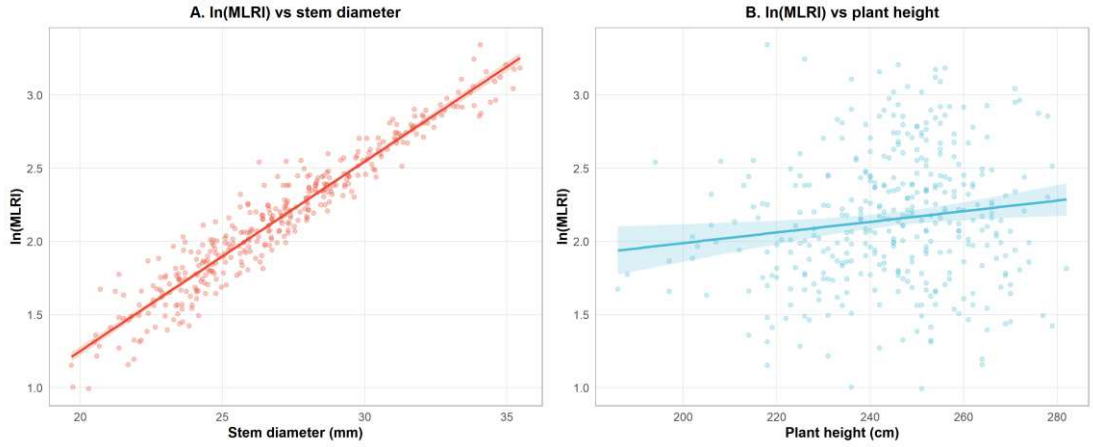


Figure S2 Relationship between ln(MLRI) and stem diameter or plant height. (A) *ln*(MLRI) versus stem diameter; (B) *ln*(MLRI) versus plant height. Solid lines represent linear fits; shaded bands represent 95% confidence intervals. Each point represents one plant-level observation (n = 370).

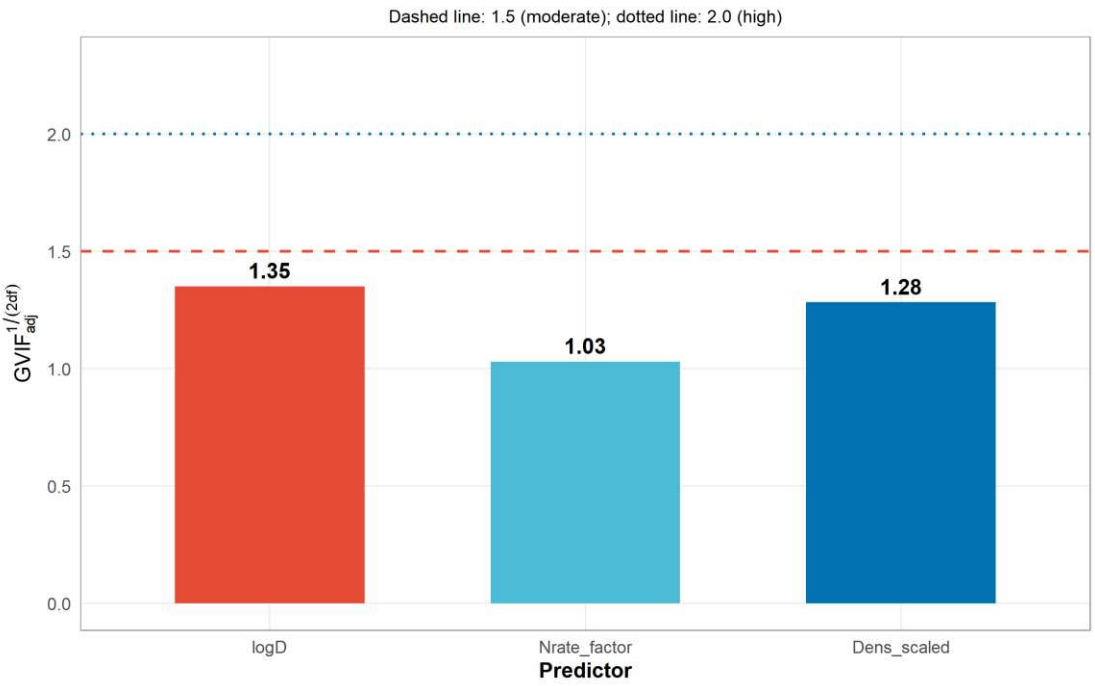


Figure S3 Multicollinearity diagnostics (VIF). Adjusted generalized variance inflation factors ($GVIF_{adj}^{\left(\frac{1}{2df}\right)}$) for the three predictors in the best-fitting mixed-effects model. The dashed line indicates the moderate collinearity threshold (1.5); the dotted line indicates the high collinearity threshold (2.0). All predictors fell below 1.5: ln(D) = 1.35, N rate = 1.03, density = 1.28.

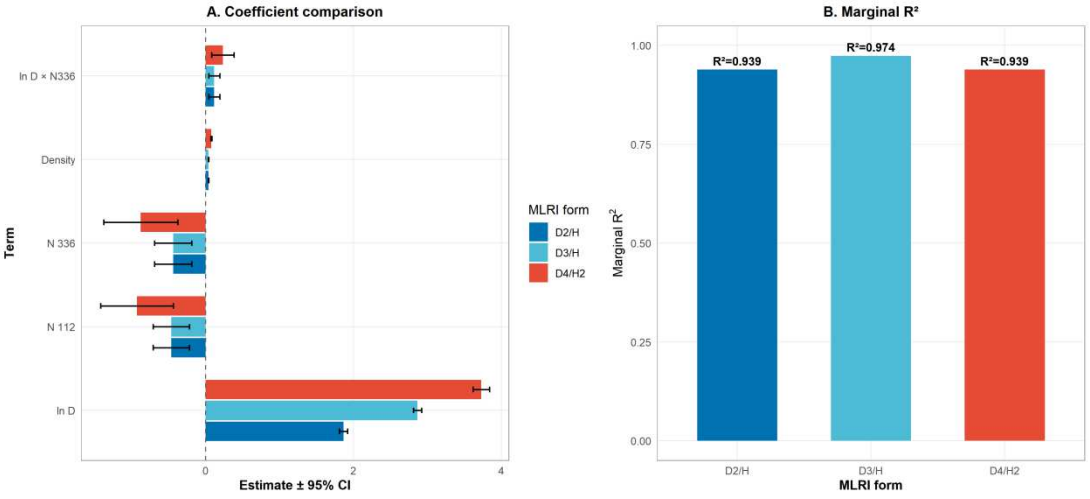
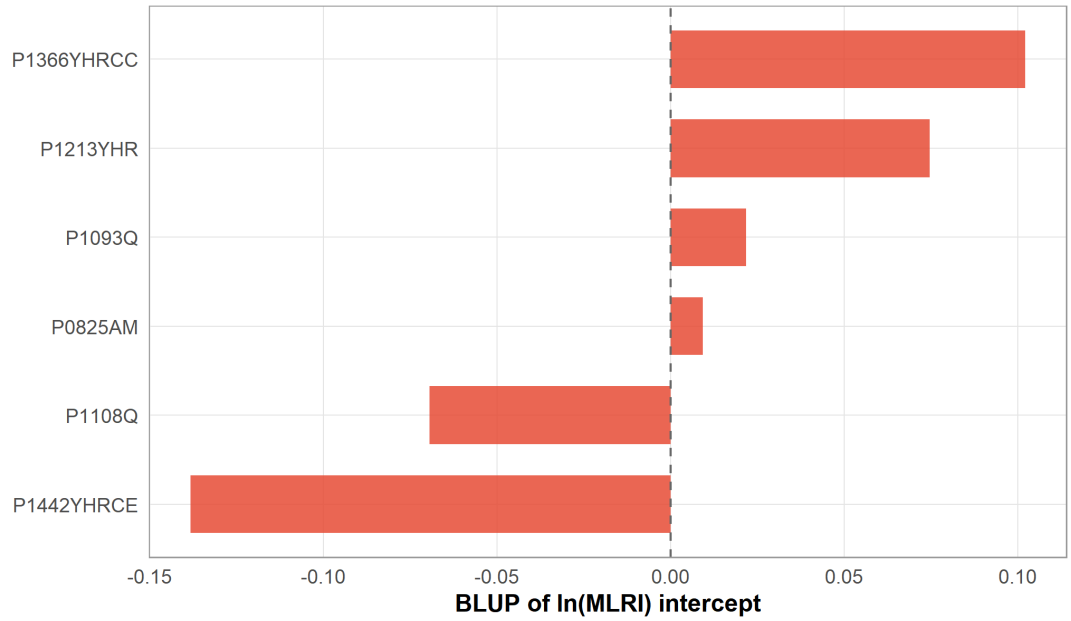


Figure S4 Sensitivity analysis across three MLRI formulations. (A) Comparison of key coefficient estimates with 95% confidence intervals across three MLRI formulations (D^4/H^2, D^3/H, D^2/H). (B) Marginal R^2 for each formulation. The significance and direction of all key coefficients were preserved across formulations,

774 confirming the robustness of the main conclusions.



775

776 **Figure S5** Hybrid BLUP values for the random intercept of ln(MLRI). Best linear
777 unbiased prediction (BLUP) values from the mixed-effects model (m4). The dashed
778 line indicates zero. Hybrids are ordered by decreasing BLUP. Because the hybrid ICC
779 was 0.671 (minimal shrinkage), BLUP values were nearly identical to the estimated
780 marginal mean deviations reported in Table 10 of the main text and are therefore
781 presented here only for completeness.